AIP Conference Proceedings

Directional plastic flow and fabric dependencies in granular materials

Barthélémy Harthong and Richard G. Wan

Citation: AIP Conf. Proc. **1542**, 193 (2013); doi: 10.1063/1.4811900
View online: http://dx.doi.org/10.1063/1.4811900
View Table of Contents: http://proceedings.aip.org/dbt/dbt.jsp?KEY=APCPCS&Volume=1542&Issue=1
Published by the AIP Publishing LLC.

Directional Plastic Flow and Fabric Dependencies in Granular Materials

Barthélémy Harthong[*] and Richard G. Wan[†]

[*]*Laboratoire 3S-R, Domaine universitaire, BP 53, 38042 Saint Martin d'Hères Cedex 9, France*
[†]*Department of Civil Engineering, University of Calgary, 2500 University Dr. NW, Calgary, Alberta T2N 1N4, Canada*

Abstract. The constitutive modelling of granular materials both at the microstructural level and the continuum level is well established. Much recent effort has been devoted to the theoretical mechanics and computer simulations of granular media through discrete element modelling (DEM). The current study uses DEM to obtain theoretical insights and extract constitutive information such as the nature of the yield and plastic flow behaviour of granular materials. In particular, we look at the influence of granular fabric on the plastic deformation response under a number of conditions. As such, a representative element volume (REV) of a granular material idealized as a numerical DEM sample is subjected to different loading paths to reach the same stress states, but with different fabrics, on the plastic failure surface. At this stage, directional stress probes of equal magnitudes are applied, so that the strain response envelopes thus obtained represent characteristics of the increment of plastic strain, i.e. the nature of the flow rule. The discussion then focuses on the relationship between fabric, stress state, loading path, direction of the plastic strain increment, and whether this direction can be considered unique or not.

Keywords: Granular Materials, Plastic Flow, Discrete Element Method, Fabric, Stress Probes, Response Envelopes.
PACS: 46

INTRODUCTION

Granular materials have been extensively studied within the field of geomechanics. Many models have been formulated, supported by complex experimental studies [1]. On the other hand, the introduction of the Discrete Element Method (DEM) [2] has enabled the numerical investigation of samples of idealized granular assemblies subjected to any kind of stress or strain path. Even though a simplified, idealized material behaviour is assumed at the particle level, DEM studies give access to almost any information on the sample, such as fabric, distribution of forces, stresses and strains.

In the present paper, the nature of plastic flow rule is studied by applying spherical stress probes on the sample at a given stress state, and thereafter determining the resulting plastic strain response envelope. Similar method has been applied in experimental studies [3] and DEM studies [4]. Spherical stress probes are stress increments of constant magnitude applied to the sample—which has been pre-loaded to a given stress state—in every direction of the 3D stress space. The response envelope is the 3D curve formed by the tips of the plastic strain increment vectors resulting from the stress probes.

A study of the relations between the direction of plastic strain and stress increments, the stress state, and the fabric tensor is proposed. It is conducted at failure conditions in the deviatoric plane. The influence of the directions of the stress increment is discussed and a micromechanical, though qualitative, interpretation is proposed for the plastic behaviour of the sample.

METHOD

The DEM code used in this study is YADE [5]. A DEM sample made of 5,000 spheres is generated in a unit cube. The constitutive behaviour of the contacts between particles is modelled by a linear force-displacement relationship, with Coulomb friction but without adhesion. The normal elastic stiffness K_n normalized to an actual particle radius is chosen as 100 MPa for a confining pressure $p = 100\text{ kPa}$, so that $K_n / p = 10^3$. The normalized shear elastic stiffness is defined as $K_s = 0.5K_n$ and the interparticle friction angle is $26°$. The numerical sample can be seen as an ensemble of polydisperse, spherical, rigid particles with negligible overlap and contacts exhibiting both elastic deformation and plastic slip.

At the end of the generation phase, the sample is compacted under isotropic loading up to a confining pressure p. At this stage, the porosity of the sample is 38%. Then, the sample is sheared at constant mean

Powders and Grains 2013
AIP Conf. Proc. 1542, 193-196 (2013); doi: 10.1063/1.4811900

pressure p along radial paths with different values of the Lode angle θ. The quasi-static state and stability of the sample are checked by computing the unbalanced force f which is the ratio of the magnitude of the sum of all contact forces to the mean force magnitude [5]. In fact, f is related to an average acceleration within the sample. A very low stress rate is used for the shearing phase, so that f is limited to a very low value of $10^{-4} \sim 10^{-5}$. Failure is detected whenever f becomes larger than a given $f_{\max} = 5\times10^{-3}$, revealing an instability inside the sample. When this criterion is met, the sample is stabilized again to $f = 10^{-5}$. These values of f ensure that the simulations remain quasi-static throughout, even close to failure.

Starting at a failure state, stress probes (112 in all) with a magnitude of 100 Pa are then applied. After a probe is applied, the sample is unloaded back to the starting point on the failure surface. As such, the resulting irrecoverable strain is obtained as the plastic strain and used to define the plastic response envelope. A fabric tensor is also calculated as an average of dyadic products of all contact normals in the sample [6].

All numerical tests presented here are performed with no rotation of the principal axes of stress. It is assumed that the stress, strain and fabric tensors remain coaxial throughout loading history, such that the state of stress, strain and fabric can be represented as a vector in a 3D space defined by the principal axes of the three tensors. This can be easily verified since the fabric tensor has diagonal components $F_{ii} \gg F_{ij,i\neq j}$.

RESULTS

Role of Stress and Fabric

The response envelopes have been normalized for a better readability, since the focus here is only on the direction of the plastic strain increment, and not its magnitude. Fig. 1 shows the computed response envelopes that are close to straight lines, suggesting that the influence of the direction of the stress increment is small compared to the influence of the stress state or fabric. The direction of the plastic strain increments is neither aligned with the direction of the stress path, nor with the normals to the failure surface.

Figure 2 shows the plastic strain response envelopes together with stress state and fabric information as a basis for further discussions. Because of particle reorganization in the sample, the fabric tensor at failure follows approximately the same trend as the stress tensor (Figs. 2*e* to 2*l*). The number of contacts oriented along a direction X_i is related to σ_i: the larger σ_i, the larger F_i. In other words, the sample reacts to the loading by creating more contacts in the direction of the largest principal stresses.

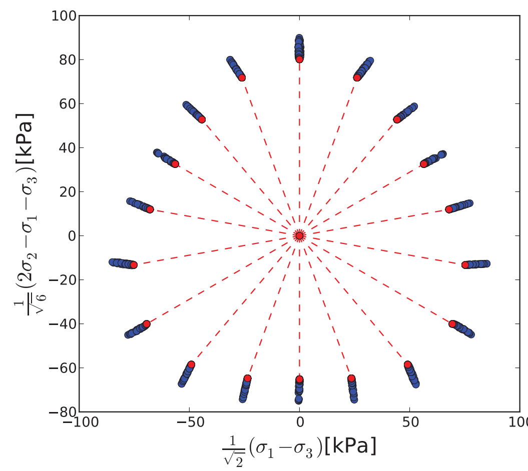

FIGURE 1. Failure envelope (in red) and response envelopes (in blue) obtained at failure along radial paths. Only one third of the deviatoric plane is computed with the other two thirds rotated from the first. However, symmetry due to isotropy can be checked on one third segment.

As a result, there is a "weak" direction on the sample, which is the direction of minor eigenvalue of the fabric tensor. The direction of the plastic strain increment cannot be directly associated with the stress state, because of the sign of the components of the principal strain increments (Figs. 2*a* to 2*d*). However, in Fig. 2, except in the case of conventional triaxial compression (CTC: $\theta = 0$, Fig. 2*a*), the largest principal strain increment always corresponds to the weakest direction of fabric—which is also the direction of minor principal stress X_1. This mechanism of plastic flow along the direction of weakest fabric/minor stress explains the non-coaxiality between the stress state and plastic strain increment vector, see [7] for instance regarding DEM.

Influence of Stress Increment

Referring back to Fig. 2, it is observed that the assumption the response envelopes can be approximated by a straight line is not exact, but is acceptable for all values of θ, except for $\theta = 0$, which is the particular case of CTC, for which the stress and fabric tensors have two equal minor eigenvalues. Therefore, there can be no preferred direction for the plastic flow.

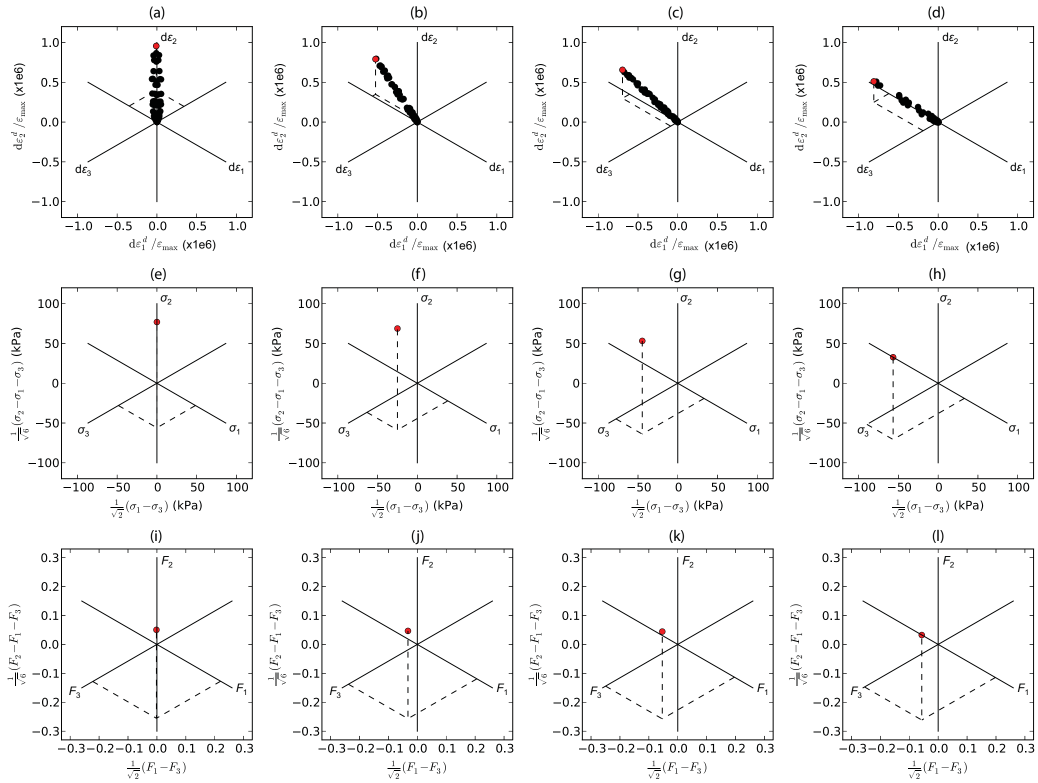

FIGURE 2. Plastic strain response envelopes (*a* to *d*), stress state (*e* to *h*) and fabric tensor (*i* to *l*) for Lode angles $\theta = 0$ (*a*,*e*,*i*); $\pi/9$ (*b*,*f*,*j*); $2\pi/9$ (*c*,*g*,*k*); $\pi/3$ (*d*,*h*,*l*). Due to isotropy of the initial sample, only one sixth of the deviatoric plane is needed to cover the whole plane, the behaviour for other Lode angles being deduced by symmetry.

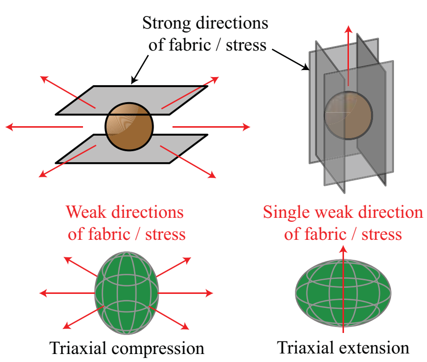

FIGURE 3. Influence of stress increment $d\sigma$ on the direction of plastic strain increment in the cases of triaxial compression and triaxial extension. The ellipsoidal surfaces illustrate the shape of the 3D fabric.

Fig. 3 illustrates, at the scale of a single average particle, assuming a distribution of contacts representative of the fabric tensor, that the deformation is not fully constrained by the fabric and stress tensors in CTC. As such, the direction of the plastic strain increment is determined by the direction of the stress increment. In all other cases, especially in triaxial extension, both the fabric and stress tensors have only one minor eigenvalue, and hence, the corresponding direction is the direction of weakness and the preferred direction for the plastic flow.

Influence of Loading Path

It was found that no difference in behaviour was noticeable when several loading paths were used to reach the isotropic state, as long as the *p*-constant radial paths between the isotropic state and failure are kept the same. This implies that any potential change in the fabric is erased by the recent history. However, there is a significant effect on the direction of the plastic strain increment when the sample is loaded with a tangent path following the failure surface. In that case, the plastic strain increment is deviated towards the direction of the loading path [8]. For each state of stress on the failure surface, the sample obtained with a radial path and with a tangent path has the same fabric tensor up to the 4th decimal place of each component. Therefore, the stress state is the same, the fabric is the same, but the plastic response is significantly different.

To clarify this mechanism, the sample was loaded with a radial path to point A (Fig. 4*a*), and then loaded with a small increment of the Lode angle θ, counter-clockwise (Fig. 4*b*, point A^+) and clockwise (Fig. 4*c*, point A^-), such that a stress increment of magnitude $d\sigma = 1$ kPa is applied.

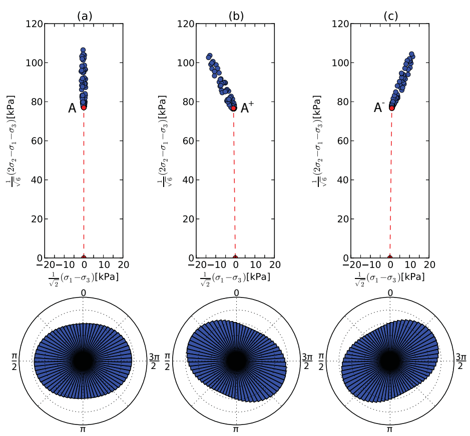

FIGURE 4. Plastic response envelope and deviatoric cross sections of the 3D fabric tensor of sliding contacts for $\theta = 0$ (a), and for a stress increment $d\sigma = 1\,\text{kPa}$ applied from case (a) counter-clockwise (b) and clockwise (c).

At points A^+ and A^-, both stress and fabric tensors are transversely isotropic, whereas the incremental strain response is purely anisotropic with respect to the previous loading history. The reason for this is friction, as suggested by the fabric tensor plots of the sliding contacts shown in Fig. 4. Here, the sliding contacts are detected as contacts for which both the normal force F_N and the tangential force F_T verify $F_T > 0.99\mu F_N$; μ being the friction coefficient. In other words, at the onset of plastic strains, only the contacts that are at limiting sliding are mobilized. This results in the plastic strain increment being deviated towards the major direction of sliding contacts. Therefore, the anisotropy of the plastic strain response is governed by the anisotropy of the distribution of these contacts that are at the sliding limit; this distribution being governed by the very last increment of stress that sets the distribution of the magnitudes of the tangential forces.

CONCLUSIONS

The paper provided a qualitative micromechanical interpretation of the mechanisms that appear between the stress increment and the plastic strain increment in an idealized, spherical, non-cohesive, elastic-frictional, dry granular material. Main conclusions are as follows.

1. For a non-cohesive assembly of spheres, the fabric tensor and the stress tensor follow the same trend. It has not been possible to obtain different fabrics for the same state of stress at failure.
2. The direction of the plastic strain increment is largely determined by the minor principal directions of stress and fabric (that were always co-linear in the present study), except in the particular case of CTC where there is no unique minor direction for stress and fabric.
3. The influence of the stress increment on the direction of the plastic strain increment is small, and more significant in the case of CTC, for which the minor direction of stress and fabric is not unique.
4. Significant anisotropy in the plastic strain response of the sample is created by the direction of the last stress increment which defines the distribution of sliding contacts that are mobilized at the onset of yielding.

ACKNOWLEDGEMENTS

This work was supported by Natural Science and Engineering Research Council of Canada (NSERC) through a Postdoctoral Fellowship to the first author.

REFERENCES

1. T. Nakai and D. Muir Wood, "Analysis of true triaxial and directional shear cell tests on Leighton Buzzard sand" in *Pre-failure deformation of geomaterials*, Shibuya, Mitachi & Miura, eds., Balkema, Rotterdam, 1994, pp. 419-425.
2. P.A. Cundall and O.D.L. Strack, *Géotechnique* **29**, 47-65 (1979).
3. D. Muir Wood, *Journal of Engineering Mechanics* **130**, 656-664 (2004).
4. F. Calvetti, G. Viggiani and C. Tamagnini, *Rivista Italiana di Geotecnica* **34**, 11-29 (2003).
5. V. Šmilauer, E. Catalano, B. Chareyre, S. Dorofeenko, J. Duriez, A. Gladky, J. Kozicki, C. Modenese, L. Scholtès, L. Sibille, J. Stransky, and K. Thoeni, *Yade Documentation*, V. Šmilauer, ed., The Yade project. 1st. ed., 2010, URL. http://yade-dem.org/doc/.
6. M. Satake, "Fabric tensor in granular materials", in *Deformation and failure of granular materials*, Vermeer and Luger eds., Balkema, Rotterdam, 1982, pp. 63-68.
7. M.H. Jiang, D. Harris and H.S. Yu, *International Journal for Numerical and Analytical Methods in Geomechanics* **29**, 663-689 (2005).
8. R. Wan and M. Pinheiro, *International Journal for Numerical and Analytical Methods in Geomechanics, under review* (2012).